Optics Letters

Simple and fully CMOS-compatible low-loss fiber coupling structure for a silicon photonics platform

Yuriko Maegami,* Makoto Okano, Guangwei Cong, Keijiro Suzuki, Morifumi Ohno, Toshihiro Narushima, Nobuyuki Yokoyama, Miyoshi Seki, Minoru Ohtsuka, Shu Namiki, and Koji Yamada

National Institute of Advanced Industrial Science and Technology (AIST), 16-1 Onogawa, Tsukuba, Ibaraki 305-8569, Japan
**Corresponding author: yuriko-maegami@aist.go.jp*

Received 15 January 2020; revised 21 February 2020; accepted 8 March 2020; posted 9 March 2020 (Doc. ID 388267); published 1 April 2020

A simple low-loss fiber coupling structure consisting of a Si inverted-taper waveguide and a 435 nm wide and 290 nm thick SiN waveguide was fabricated with fully complementary metal-oxide semiconductor (CMOS)-compatible processes. The small SiN waveguide can expand to the optical field corresponding to a fiber with a mode-field diameter of 4.1 μm. The fiber-to-chip coupling losses were 0.25 and 0.51 dB/facet for quasi-TE and quasi-TM modes, respectively, at a 1550 nm wavelength. Polarization-dependent losses of the conversion in the Si-to-SiN waveguide transition and the fiber-to-chip coupling were less than 0.3 and 0.5 dB, respectively, in the wavelength range of 1520–1580 nm.

https://doi.org/10.1364/OL.388267

An interminable challenge we face in bringing silicon (Si) photonics platforms into practical use is how to realize a Si waveguide structure that efficiently couples with an optical fiber, while keeping the compatibility with the standard complementary metal-oxide semiconductor (CMOS) fabrication. The core dimensions of a Si waveguide are significantly smaller than those of a typical optical fiber. Therefore, the coupling loss is large due to mode-field mismatch. Among many approaches to solving issues on coupling between the optical fiber and Si waveguide, or fiber-to-chip coupling, grating couplers and edge couplers are generally implemented [1–15]. Grating couplers are attractive as wafer-level testing using single-mode fibers, but usually suffer from a small bandwidth and strong polarization dependence for coupling efficiency [1–3]. On the other hand, double-core fiber-chip edge coupling structures consisting of a Si inverted-taper waveguide and some secondary waveguides made of a low-refractive-index material are widely used because they provide high-efficiency, low-polarization dependence and wide-bandwidth optical coupling (see for example [3–15]). High numerical-aperture (NA) single-mode fibers and/or lensed fibers are widely used for coupling with the edge couplers in order to best match the mode fields. The high NA fiber, in particular, has already been in production worldwide and is becoming popular in the market. Its mode-field diameter (MFD) is typically around 4 μm at the wavelength of 1550 nm. It is worthwhile to design fiber coupling structures that efficiently couple with such a fiber. In the double-core structures, the optimum core dimensions of the secondary waveguide, such as the one made from silicon-rich silica [4–6], silicon oxynitride (SiON) [7–9], and alternately stacked silicon nitride and silicon dioxide (SiN/SiO_2) [10], are determined, depending on the MFD of the optical fiber. Since the core dimensions can reach several micrometers, thick-film deposition and etching are required, which are not supported in standard CMOS processes. Moreover, a thick secondary core is incompatible with multiple metal layers for flexible electronic interconnects. A SiN waveguide-based edge coupler fabricated by CMOS-compatible processes [11] provided low-loss interlayer transition, but would be required further improvement in optical coupling because the optical field at the edge is tightly confined in the core. A multi-rod coupling structure composing multiple SiN secondary waveguides [12] might increase the effective core size of the secondary waveguide and allow electronic interconnect layers to be inserted between SiN layers. However, this approach involves very complicated processes, which decrease manufacturing efficiency considerably. In addition, a total thickness of the multi-rod coupling structure is beyond those allowed in standard CMOS process, where sub-micrometer-size structures, such as multilayer electronic interconnections and Si/SiN photonic waveguides, should be fabricated in a few micrometer thick layer (2–3 μm) [16]. Although a thinner coupling structure based on an inverted-taper secondary SiN waveguide is also proposed [13], it requires a non-CMOS-compatible process for undercutting the Si handle wafer to prevent an optical leakage into the substrate. As a simpler and fully CMOS-compatible fiber coupling structure, we previously proposed one using a thin SiN waveguide with very weak optical confinement, which can efficiently expand the optical field [15].

In this Letter, we fabricated this fiber coupling structure by the in-house 300 mm wafer standard CMOS processes with ArF immersion and KrF lithography, and confirmed, to the best of our knowledge, the lowest coupling loss ever reported, and low-polarization dependence.

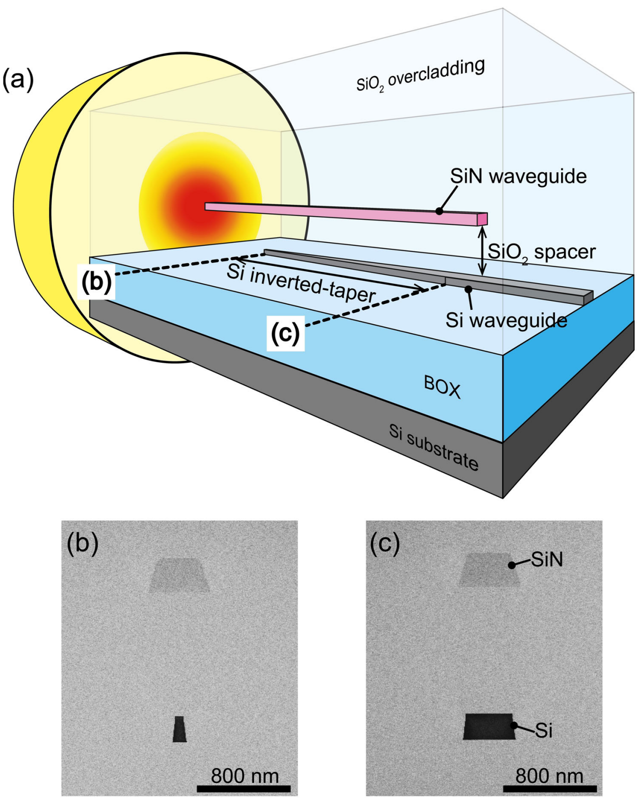

Fig. 1. Demonstrated fiber coupling structure: (a) schematic diagram; (b) and (c) cross-sectional STEM images.

Figure 1(a) shows the schematic diagram of the fiber coupling structure. It consists of a thin SiN waveguide and a Si inverted-taper waveguide with a SiO_2 spacer layer inserted between them. The SiN waveguide has a very small sub-micrometer core, which can expand the optical field enough for efficient fiber coupling. The optical field enlarged in the SiN waveguide can be adiabatically transferred to a Si waveguide through the Si inverted-taper waveguide. Moreover, the SiO_2 spacer can suppress the optical leakage into the Si substrate, because the SiN waveguide is away from the substrate. The structural design is mainly based on that in our previous work [15]. However, the structural design should be modified so as to satisfy the process guidelines of a fully CMOS-compatible fabrication process. To keep from damaging the photonic and electronic device built-in SOI layer, the SiN film should be deposited by low-temperature plasma-enhanced chemical vapor deposition (PECVD), and the thickness of the SiN film should be around or less than 300 nm. Moreover, the refractive index of the SiN film deposited by PECVD is generally lower than that of a stoichiometric SiN, and is around 1.93 for our SiN film. Taking these realistic parameters into consideration, we determined that the width and thickness of the SiN waveguide should be 400 and 280 nm, respectively, which provides efficient fiber-to-chip coupling for an MFD of 4.1 μm for both the quasi-TE and quasi-TM modes.

To experimentally examine the device performance with relation to the fiber-to-chip coupling, we fabricated the fiber coupling structure using a 300 mm wafer fully CMOS-compatible process. First, the Si waveguide was fabricated on the SOI substrate with a 3 μm thick buried oxide layer by using ArF immersion lithography in which a standard deviation of line width is less than 1 nm on an entire wafer surface [17]. The typical core width and thickness are 440 and 220 nm, respectively. The length of the Si inverted-taper is 300 μm, and the tip width is 80 nm. These taper length and tip width of the Si waveguide can guarantee the efficient conversion at a waveguide transition. Next, the SiO_2 spacer layer was deposited by low-temperature PECVD, and its thickness was reduced to around 1 μm by chemical mechanical polishing. After that, a SiN film was formed by low-temperature PECVD. The SiN waveguide was fabricated by KrF lithography. Finally, the SiN waveguide was covered with a 3 μm thick SiO_2 overcladding. Figures 1(b) and 1(c) show scanning transmission electron microscopy (STEM) images of cross sections of the fiber coupling structure around the Si inverted-taper tip [marked by (b)] and the Si waveguide [marked by (c)], respectively. The tip and typical core widths of the Si waveguide are almost the same as those in the design. The thickness of the fabricated SiN core is 290 nm. The SiN waveguide has a trapezoid core, in which the upper and lower base widths are 340 and 530 nm, respectively, with an average of 435 nm. Although a few tens of nanometer fabrication errors exist, they would have almost no influence on device performance because of the large fabrication margins in the design [15].

The fabricated device wafer was diced into separate chips by stealth laser dicing and breakage. Infrared light emitted from an amplified spontaneous emission light source was guided by a single-mode fiber into a polarization controller to determine the quasi-TE and quasi-TM modes. For external optical coupling to a Si photonics chip, a high NA single-mode fiber with an MFD of 4.1 μm can be used, which can connect to an ordinary single-mode fiber with an optical loss of less than 0.1 dB by applying a thermal expansion core technology [14]. Each polarized light was fed into the Si waveguide by butt-coupling between the optical fiber and the SiN waveguide at the chip edge. In addition, to eliminate reflection and scattering losses at a slight air gap between them, the gap was filled with a matching oil whose refractive index is 1.45 at the wavelength of 1550 nm. The wavelength of the guided light ranged from 1520 to 1580 nm, which includes wavelengths in the C band. We measured the transmission properties of the Si waveguide with the fiber coupling structure using an optical spectrum analyzer. The measured spectra were normalized by the spectrum of the butt-coupling between the input and output fibers. All the Si waveguides composed 20 waveguides bent at 90° with a 20 μm radius. The 90° bend losses at the wavelength of 1550 nm were 0.007 and 0.017 dB/bend for the quasi-TE and quasi-TM modes, respectively, and the wavelength dependence was slight. Therefore, we subtracted the spectra of the total loss of the 20 bends from the measured transmission spectra.

To evaluate the propagation losses of the Si waveguide and the fiber-to-chip coupling losses, we used a standard cut-back method with different Si waveguide lengths. Figure 2(a) shows the transmittance of the Si waveguides with respect to waveguide length. The transmittance was averaged in the wavelength range of 1550–1551 nm, and bending losses were subtracted. The propagation losses of the Si waveguide are 0.9 and 1.5 dB/cm for the quasi-TE and quasi-TM modes, respectively. The vertical intercept of the linear fitting represents the coupling loss between the fiber and the Si waveguide for the two facets. Therefore, the fiber-to-chip coupling losses

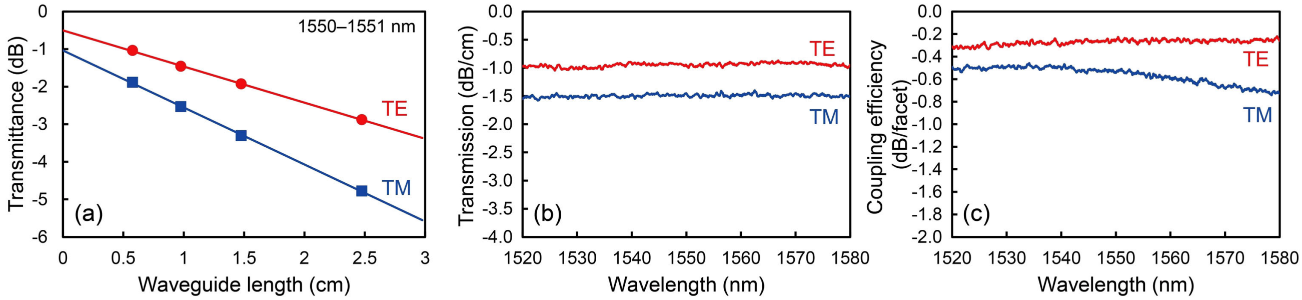

Fig. 2. (a) Transmittance of the Si waveguide as a function of waveguide length, (b) spectra of transmission per length, and (c) spectra of fiber-to-chip coupling efficiency.

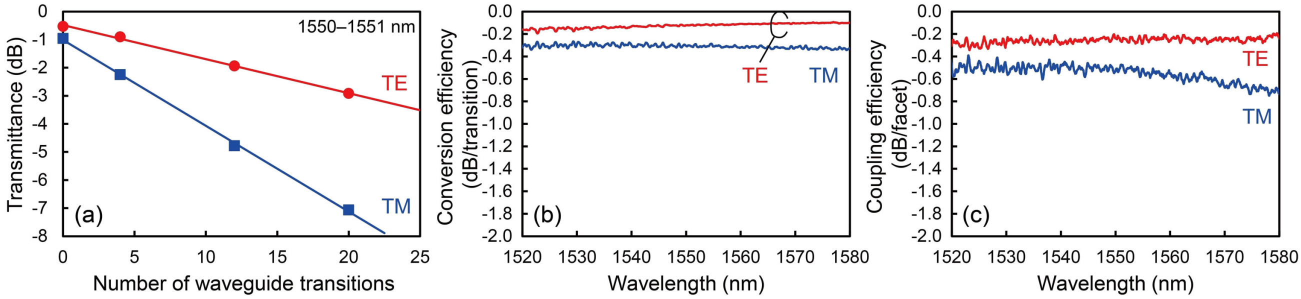

Fig. 3. (a) Transmittance of the Si waveguide with a number of waveguide transitions, (b) spectra of conversion efficiency at Si-to-SiN waveguide transition per transition, and (c) spectra of fiber-to-chip coupling efficiency.

per facet are estimated to be 0.25 and 0.51 dB for the quasi-TE and quasi-TM modes, respectively. By applying the same evaluation procedure to the entire measured spectral range, we evaluated the wavelength dependence of the coupling efficiency. Figure 2(b) shows propagation losses, which are around 1.0 and 1.5 dB/cm for the quasi-TE and quasi-TM modes, respectively, and remain flat over the wavelength range of 1520–1580 nm. Figure 2(c) shows the fiber-to-chip coupling efficiency evaluated from the results of the waveguide cutback measurement. The coupling losses for the quasi-TE and quasi-TM modes are less than 0.3 and 0.7 dB/facet, respectively, in the wavelength range of 1520–1580 nm.

Moreover, we evaluated the temperature dependence of transmission losses. The temperature range in the measurement was 10–70°C, and the wavelength range was 1550–1551 nm. The experimental results demonstrated that the propagation losses of the Si waveguide were insensitive to the temperature, and the fiber-to-chip coupling losses slightly varied. The variation of coupling losses was less than ±0.1 dB with respect to the room temperature reference (25°C), and we have confirmed a very small temperature dependence of the device performance.

The fiber-to-chip coupling loss includes conversion loss at the Si-to-SiN waveguide transition and coupling loss between the SiN waveguide and fiber. To break down the losses in detail, we evaluated the conversion loss at the Si-to-SiN waveguide transition using Si waveguides arranged in different numbers of conversion structures. Figure 3(a) shows the transmittance of Si waveguides with respect to the number of waveguide transitions. The transmittance was averaged in the wavelength range of 1550–1551 nm. Propagation and bending losses in the Si waveguide were also subtracted. Estimated conversion losses per transition are 0.12 and 0.31 dB for the quasi-TE and quasi-TM modes, respectively. The vertical intercept of the linear fitting in Fig. 3(a) also represents the fiber-to-chip coupling loss for the two facets. The fiber-to-chip coupling losses per facet are estimated to be 0.24 and 0.51 dB for the quasi-TE and quasi-TM modes, respectively. These fiber-to-chip coupling losses completely agree with the ones estimated by the cutback method [see Fig. 2(a)].

Here we compared these experimental results with calculated ones for the designed fiber coupling structure. The calculated conversion losses per transition are obtained to be 0.12 and 0.32 dB for the quasi-TE and quasi-TM modes, respectively, and they almost agree with the experimental results. The calculated fiber-to-chip coupling losses per facet are obtained to be 0.30 and 0.42 dB for the quasi-TE and quasi-TM modes, respectively. The slight variation of less than ±0.1 dB might be caused by the trapezoid core of the SiN waveguide and the optical leakage into the Si substrate. A few tens of nanometer fabrication error did not influence the device performance.

Figure 3(b) shows the spectra of conversion loss at Si-to-SiN waveguide transition per transition, which are less than 0.2 and 0.4 dB for the quasi-TE and quasi-TM mode, respectively, in the wavelength range of 1520–1580 nm. Figure 3(c) shows the fiber-to-chip coupling efficiency evaluated from the results of the conversion loss measurement. The results in Fig. 3(c) are almost the same as those evaluated from the waveguide cutback measurement [see Fig. 2(c)]. Although the spectra in Figs. 2(c) and 3(c) have similar noise structures, these noises mainly originate from the ones of the propagation and bending losses commonly subtracted in coupling efficiency derivation. The coupling losses for the quasi-TE and quasi-TM modes are less than 0.3 and 0.7 dB/facet, respectively, in the wavelength range of 1520–1580 nm.

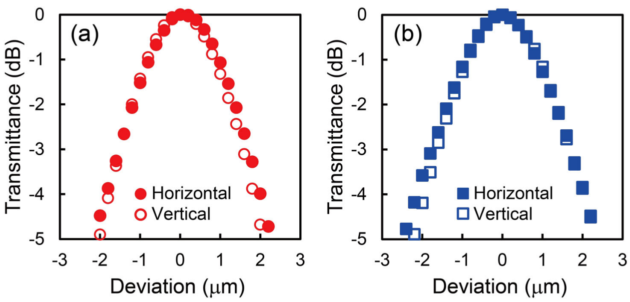

Fig. 4. Results of alignment tolerance measurement for the (a) TE mode and (b) TM mode.

From these results, we estimated the polarization-dependent loss (PDL) of the conversion in the waveguide transition and the fiber-to-chip coupling to be less than 0.3 and 0.5 dB, respectively, in the measurement wavelength range. The conversion loss for the quasi-TM mode is slightly larger than that for the quasi-TE mode because the tip of the Si inverted-taper is too wide (80 nm). The PDL of fiber-to-chip coupling is larger than that of conversion in waveguide transition at wavelengths above 1560 nm. In this wavelength range, mode mismatch between the fiber and the SiN waveguide might contribute to the PDL.

We also measured the fiber alignment tolerances, which are shown in Fig. 4. The input optical fiber was moved in the horizontal or vertical direction, while the output fiber was kept in alignment. The 1 dB alignment tolerances in the horizontal and vertical directions are approximately ±0.9 μm for both polarization modes.

To confirm a feasibility of the fiber coupling structure to a standard single-mode fiber with a 10 μm MFD, we evaluated the fiber-to-chip coupling losses for a SMF-28. The coupling structure was the same as those designed for a 4.1 μm MFD. The fiber-to-chip coupling losses were estimated to be 2.9 and 2.1 dB/facet for the quasi-TE and quasi-TM modes, respectively. A numerical calculation suggested that the fiber-to-chip coupling loss is mainly determined by the coupling between the fiber and the SiN waveguide, and indicated that it can be reduced to less than 0.7 dB by reducing the core size of the SiN waveguide to 320 nm wide and 280 nm thick. Therefore, optimization of structural parameters, such as the tip width and length of the Si taper waveguide and spacer thickness, and careful treatment of optical leakage into the Si substrate would make this extremely simple structure applicable to the coupling of a fiber with a 10 μm MFD.

In conclusion, as an efficient, practical, and fully CMOS-compatible fiber-to-chip coupling structure for Si photonics platforms, we experimentally demonstrated a low-loss and low-polarization-dependent coupling structure consisting of a small SiN waveguide and Si inverted-taper waveguide. For the single-mode fiber with a 4.1 μm MFD, the fiber-to-chip coupling losses at the wavelength of 1550 nm are 0.25 and 0.51 dB/facet for the quasi-TE and quasi-TM modes, respectively. Moreover, the applicable bandwidth exceeds 60 nm with a coupling loss of less than 0.7 dB maintained.

Disclosures. The authors declare no conflicts of interest.

REFERENCES

1. F. V. Laere, G. Roelkens, M. Ayre, J. Schrauwen, D. Taillaert, D. V. Thourhout, T. F. Krauss, and R. Baets, J. Lightwave Technol. **25**, 151 (2007).
2. A. Mekis, S. Gloeckner, G. Masini, A. Narasimha, T. Pinguet, S. Sahni, and P. D. Dobbelaere, IEEE J. Sel. Top. Quantum Electron. **17**, 597 (2011).
3. R. Marchetti, C. Lacava, L. Carroll, K. Grandkowski, and P. Minzioni, Photonics Res. **7**, 201 (2019).
4. B. B. Bakir, A. Vazquez de Gyves, R. Orobtchouk, P. Lyan, C. Porzier, A. Roman, and J.-M. Fedeli, IEEE Photonics Technol. Lett. **22**, 739 (2010).
5. T. Tsuchizawa, K. Yamada, T. Watanabe, S. Park, H. Nishi, R. Kou, H. Shinojima, and S. Itabashi, IEEE J. Sel. Top. Quantum Electron. **17**, 516 (2011).
6. M. Tokushima, H. Kawashima, T. Horikawa, and K. Kurata, J. Lightwave Technol. **36**, 4783 (2018).
7. T. Tsuchizawa, K. Yamada, H. Fukuda, T. Watanabe, J. Takahashi, M. Takahashi, T. Shoji, E. Tamechika, S. Itabashi, and H. Morita, IEEE J. Sel. Top. Quantum Electron. **11**, 232 (2005).
8. H. Park, S. Kim, J. Park, J. Joo, and G. Kim, Opt. Express **21**, 29313 (2013).
9. Y. Maegami, R. Takei, E. Omoda, T. Amano, M. Okano, M. Mori, T. Kamei, and Y. Sakakibara, Opt. Express **23**, 21287 (2015).
10. N. Kohli, M. Ménard, and W. N. Ye, OSA Contin. **2**, 2428 (2019).
11. Y. Huang, J. Song, X. Luo, T.-Y. Liow, and G.-Q. Lo, Opt. Express **22**, 21859 (2014).
12. M.-J. Picard, Y. Painchaud, C. Latrasse, C. Larouche, F. Pelletier, and M. Poulin, *European Conference on Optical Communication (ECOC)* (2015), paper Mo.4.2.4.
13. B. Snyder, G. Lepage, S. Balakrishnan, P. D. Heyn, P. Verheyen, P. Absil, and J. V. Campenhout, *IEEE CPMT Symposium Japan (ICSJ)* (IEEE, 2017), pp. 55–58.
14. T. Shoji, T. Watanabe, K. Yamada, and H. Morita, Electron. Lett. **38**, 1669 (2002).
15. Y. Maegami, M. Okano, G. Cong, M. Ohno, and K. Yamada, Opt. Express **24**, 16856 (2016).
16. K. Fischer, M. Agostinelli, C. Allen, D. Bahr, M. Bost, P. Charvat, V. Chikarmane, Q. Fu, C. Ganpule, M. Haran, M. Heckscher, H. Hiramatsu, E. Hwang, P. Jain, I. Jin, R. Kasim, S. Kosaraju, K. S. Lee, H. Liu, R. McFadden, S. Nigam, R. Patel, C. Pelto, P. Plekhanov, M. Prince, C. Puls, S. Rajamani, D. Rao, P. Reese, A. Rosenbaum, S. Sivakumar, B. Song, M. Uncuer, S. Williams, M. Yang, P. Yashar, and S. Natarajan, *IEEE International Interconnect Technology Conference and 2015 IEEE Materials for Advanced Metallization Conference (IITC/MAM)* (IEEE, 2015), pp. 5–8.
17. T. Horikawa, D. Shimura, H. Okayama, S.-H. Jeong, H. Takahashi, J. Ushida, Y. Sobu, A. Shiina, M. Tokushima, K. Kinoshita, and T. Mogami, IEEE J. Sel. Top. Quantum Electron. **24**, 8200415 (2018).